# One-Dimensional Polymers and Mesogens Incorporating Multiple Bonds between Metal Atoms

MALCOLM H. CHISHOLM
*Department of Chemistry, Indiana University, Bloomington, Indiana 47405*

Received May 27, 1999

**ABSTRACT**
A synthetic strategy aimed at incorporating metal−metal multiple bonds into one-dimensional polymers and liquid crystals is outlined. Specific examples taken from the use of dimetal tetracarboxylates, where the metals are molybdenum and tungsten, are presented. Depending upon the organic linking group, the one-dimensional polymers may be conducting or charge-storing, and the characterization of discrete dimers of "dimers" is used to illustrate this. The thermotropic and other physicochemical properties of mesogenic $M_2(O_2CR)_4$ compounds can be related to the intermolecular $M_2$- - -O interactions as a function of M and R.

The synthesis and utilization of polymers and liquid crystals (mesogens) have transformed the way in which we live. This new world of polymeric and liquid crystalline materials is primarily organic, being dominated by the use of the elements carbon, hydrogen, oxygen, nitrogen, and, to a lesser extent, some neighboring main group elements such as boron, silicon, phosphorus, and sulfur. The metallic elements, which comprise more than half of the elements in the Periodic Table, have thus far contributed virtually nothing of fiscal value to the field of polymers or liquid crystals beyond their occasional use in the catalysis by which polymers are formed. It seems that this situation might change in the years to come, as metal ions have attractive features for new generations of metalloorganic polymers and metallomesogens, polymers, and liquid crystalline materials that contain metal ions.[1] Metal ions may exhibit specific coordination preferences, may be redox active, may have unpaired electrons, may be photosensitive, and may, in innumerable ways, be anticipated to modify an organic polymer or mesogen. As two limiting situations, they may be present as guests or they may be the architects and engineers of a polymer or mesogen.

With these simple ideas, we set forth in 1989 to incorporate dinuclear ($M_2$) units containing M−M multiple bonds into one-dimensional polymers[2] and mesogens.[3] Since Cotton's recognition of the M−M quadruple bond in 1964, the field of multiple bonds between metal atoms has been one of the active areas of modern coordination chemistry[4] and, indeed, continues to draw attention from those interested in reactivity, structure, and bonding, as can be seen from the recent discourse on the Ga−Ga triple bond.[5]

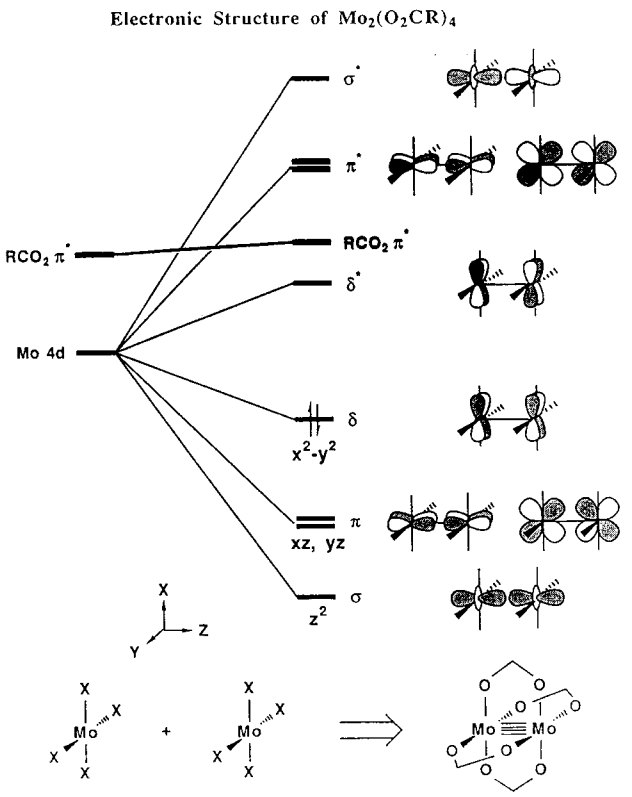


**FIGURE 1.** Electronic description of the frontier molecular orbitals in $M_2(O_2CR)_4$ compounds.

As an entry point into this new area of chemistry, we elected to work with dimetal carboxylates, $M_2(O_2CR)_4$, of molybdenum and tungsten.[4] These have the paddle-wheel molecular structure depicted by **A**. Their electronic structure has been extensively studied, and the essential feature of their M−M electronic configuration is depicted in Figure 1. By selection of M (Mo vs W) and R (R = alkyl, aryl, $CF_3$), the redox properties of the $M_2$ center can be tuned by 2 V for the solution reaction $M_2(O_2CR)_4 \rightarrow M_2(O_2CR)_4^+ + e^-$. A similar trend of ionization energies (in electronvolts) is seen in the gas-phase photoelectron spectra of the volatile compounds $M_2(O_2CR)_4$, where M = Mo, W and R = $^t$Bu and $CF_3$.[6] The singlet $\delta \rightarrow \delta^*$ electronic transition for M = Mo and R = Me or $^t$Bu, occurs at 436 nm ($\epsilon \approx 100$) and the $\delta \rightarrow CO_2\ \pi^*$ (MLCT)

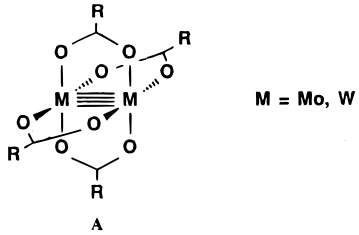


**A**

Malcolm H. Chisholm is currently Distinguished Professor of Mathematical and Physical Sciences at The Ohio State University. He was the 1999 recipient of the ACS Award for Distinguished Service to Inorganic Chemistry and the Davy Medal of the Royal Society, London. He is the Y2K recipient of the Ludwig Mond Lectureship and Medal of the Royal Society of Chemistry, United Kingdom. Born in Bombay, India, to Scottish parents, he was educated in England (Canford School; London University, B.S., 1966; Ph.D., 1969). He has taught at Princeton and Indiana University and has research interests in inorganic, organometallic, and materials chemistry.

10.1021/ar9800901 CCC: $19.00 
Published on Web 12/21/1999

transition occurs at higher energy, 296 nm ($\epsilon \approx 10\,000$).[7] For R = aryl and *p*-$NO_2$-$C_6H_4$, the $\delta \rightarrow CO_2\ \pi^*$ transition is significantly shifted ($\lambda_{max} \approx 600$ nm for R = $C_6H_4$-*p*-$NO_2$) and completely masks the weak $\delta \rightarrow \delta^*$ transition.[8] For M = W, the higher orbital energy of the $\sigma^2\pi^4\delta^2$ manifold results in the $\delta \rightarrow CO_2\ \pi^*$ transition occurring at 377 nm ($\epsilon \approx 13\,000$), and the $\delta \rightarrow \delta^*$ transition is again masked.[9]

Two further points of interest concerning the M−M quadruple bonds are worthy of mention before we examine their role in "ordered assemblies". (1) They have a very large magnetic anisotropy, larger than that of a carbon−carbon triple bond but similar in nature.[10] (2) They exhibit a huge third-order nonlinear optical susceptibility.[11] Again, this is similar in nature to that of a C−C triple or double bond but is an order of magnitude larger in the value of $\gamma$.

## One-Dimensional Polymers

**Syntheses.** Two limiting types of one-dimensional polymers can be envisaged, and these are shown in the drawings **B** and **C**.

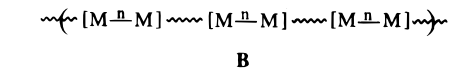


**B**

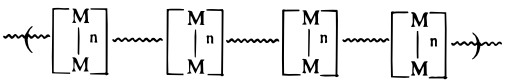


**C**

In **B**, the M−M axis associated with the M−M bond of order *n* is parallel to the propagating axis, whereas in **C** the M−M axis is perpendicular. Control of the orientation of the M−M axis and the polymer propagation rests on the judicious selection of bridging ligands, denoted in **B** and **C** by the squiggly line.

Synthesis of polymeric materials of types **B** and **C** can be achieved by a carboxylate exchange reaction, as shown in eq 1, where −R− represents a rigid rod spacer.[12] Our

$$M_2(O_2C^tBu)_4 + HOOC{-}R{-}COOH \rightarrow {}^1/_n\,[M_2(O_2C^tBu)_2(O_2C{-}R{-}CO_2)]_n + 2^tBuCOOH \quad (1)$$

initial choice of the pivalates was made simply because the Me protons provide a good $^1$H NMR signature and the $^t$Bu group provides for better solubility than the acetate derivatives. However, an increase in the solubility of the polymers can be achieved with the use of long-chain *n*-alkyl carboxylates such as *n*-octanoate, $CH_3(CH_2)_6CO_2^-$. Reaction 1 is an equilibrium reaction, and in order to drive the reaction to the right the pivalic acid must be removed, e.g., as an azeotrope, or the dicarboxylic acid HOOC−R−COOH must be more acidic than pivalic acid. The latter pertains to the use of oxalic acid and perfluoroterephthalic acid.

Hydrocarbon-soluble oligomers derived from $Mo_2(O_2C^tBu)_4$ have been obtained with ca. 10 $Mo_2$ units, as judged by molecular weight determinations.[12] The end groups, as determined by NMR spectroscopy, are either $^t$BuCO$_2$ or free COOH groups derived from HOOC−R−COOH. Again, by NMR spectroscopy, the substitution pattern appears to be predominantly trans, thus generating a linear oligomer of the type shown in **D**.

$$-[Mo_2]-O_2C-R-CO_2-[M_2]-O_2C-R-CO_2-[M_2]-$$

**D**

For oxalate and R = $C_6F_4$, these are perpendicular polymers of the general type denoted by **C**, and, by judicious choice of stoichiometry and reaction conditions in reaction 1, model compounds $(Bu^tCO_2)_3M_2(O_2C{-}R{-}CO_2)M_2(O_2C^tBu)_3$ can be isolated.[12] These afford the opportunity to study the nature of the electronic coupling between the bridged $M_2$ centers. Recently, Cotton, Lin, and Murillo[13] have reported the single-crystal X-ray molecular structure for oxalate- and perfluoroterephthalate-linked formamidinate analogues. These linked dimers of "dimers" provide excellent models for subunits within the stiff-chain polymers.

The use of 1,8-anthracenedicarboxylic acid in reaction 1 affords a parallel polymer of type **B**. Similarly, the metathetic reaction shown in eq 2, where L is a labile solvent ligand such as $CH_3CN$ and $Q^+ = Bu_4^nN^+$ or $Na^+$, affords an alternate procedure for the synthesis of linked dimers of "dimers" in extended arrays.[12]

$$Mo_2(O_2C^tBu)_2L_4^{2+}(BF_4^-)_2 + Q^+_2(bridge^{2-}) \rightarrow {}^1/_n\,[Mo_2(O_2C^tBu)_2(bridge)]_n + 2QBF_4 \quad (2)$$

The use of a bridging ligand such as the anion derived from 2,7-dihydroxynaphthyridine gives a polymer of the type shown in **E**.[2a,12] Once again, a model for a subsection

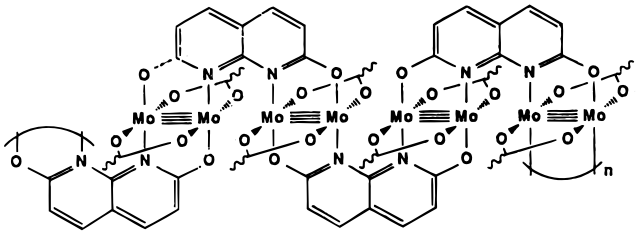

**E**

of this polymer can be obtained by the preparation of a simple dimer of "dimers" according to eq 3.[12]

$$2Mo_2(O_2C^tBu)_3L_2^+BF_4^- + Na_2O_2C_8N_2H_4 \xrightarrow[\text{THF/MeOH}]{0^\circ C}$$

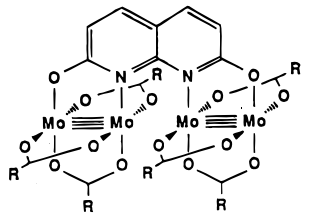

(R = $^t$Bu) (3)

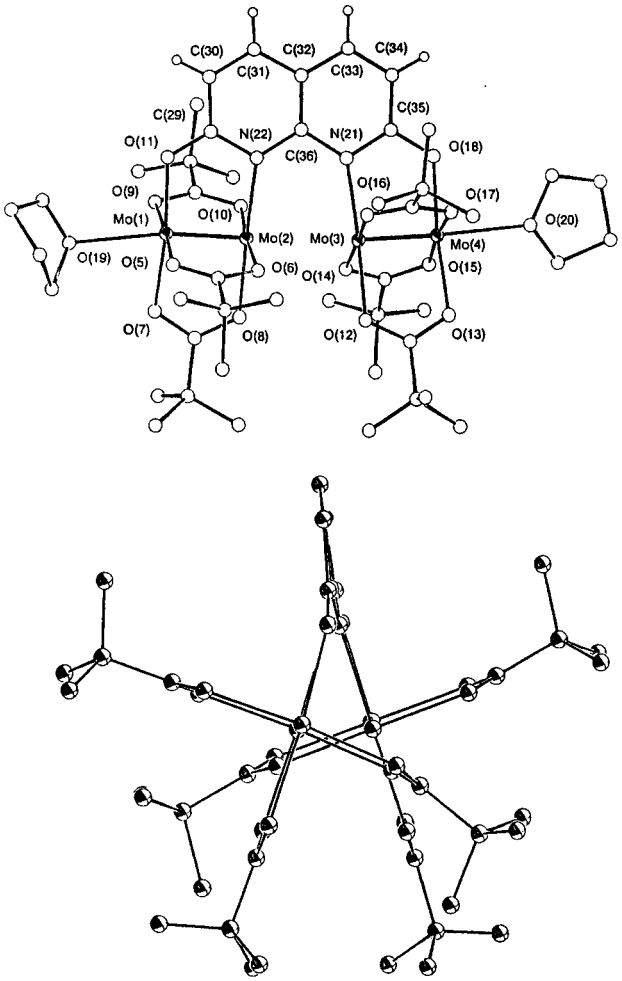


**FIGURE 2.** Molecular structure of a 2,7-dioxynaphthyridine-linked dimer of "dimers" viewed perpendicular to the M−M axes (top) and along the M−M axes (bottom).

The molecular structure of this linked dimer of "dimers" is shown in Figure 2 and is instructive with respect to the nature of the polymer shown in drawing **E**.

As shown in **E**, there are unfavorable O- - -O interactions of 2.4 Å involving carboxylates of neighboring $M_2$ units. A slight ruffling of the 2,7-dioxynaphthyridine ligand releaves these repulsive O- - -O interactions and leads to a significant displacement of the trans $O_2C^tBu$ ligands, as can be seen at the bottom of Figure 2. The linked dimer of "dimers" has $C_2$ symmetry in the ground state, but in solution the molecule has time-averaged planar symmetry on the $^1H$ and $^{13}C$ NMR time scale at room temperature.[12] Below −60 °C, however, the $C_2$ symmetry becomes frozen out on the NMR time-scale. So, from an inspection of the structure of the dimer of "dimers" (Figure 2), it becomes apparent that polymer propagation is favored in order to relieve these otherwise unfavorable O- - -O interactions. The same situation pertains to 1,8-anthracenedicarboxylate-linked dimers of "dimers" and their oligomers, though here twisting about the anthracene 1- and 8-carbon to carboxylate carbon bonds is also possible.[12]

**Electronic Structures.** From the hydrocarbon-insoluble polymers derived from reaction 2, it is apparent that there must be significant interaction between the $M_2$ centers. The $M_2(O_2C^tBu)_4$ complexes are yellow, whereas the oxalate-bridged polymers are maroon (M = Mo) and purple-black (M = W).[12] Once again, studies of the linked "dimers" are instructive in ascertaining the nature of the bonding in the polymers.

The electronic spectrum of the oxalate-bridged dimers of "dimers" is shown in Figure 3 for M = Mo and W. These red and purple compounds show very strong bands, $\epsilon \approx$ 10 000 (M = Mo), $\epsilon \approx$ 30 000 (M = W), in the visible region which cannot be assigned to $M_2$ $\delta \rightarrow O_2C$ $\pi^*$ (pivalate) transitions, but rather must be assigned to $\delta \rightarrow$ oxalate $\pi^*$ transitions. The oxalate-bridged $[W_2]_2$ complex shows $\lambda_{max} \approx$ 700 nm with a vibronic progression of ca. 1500 $cm^{-1}$. A low-temperature visible spectrum of the $[Mo_2]_2$ complex reveals a similar progression.[14]

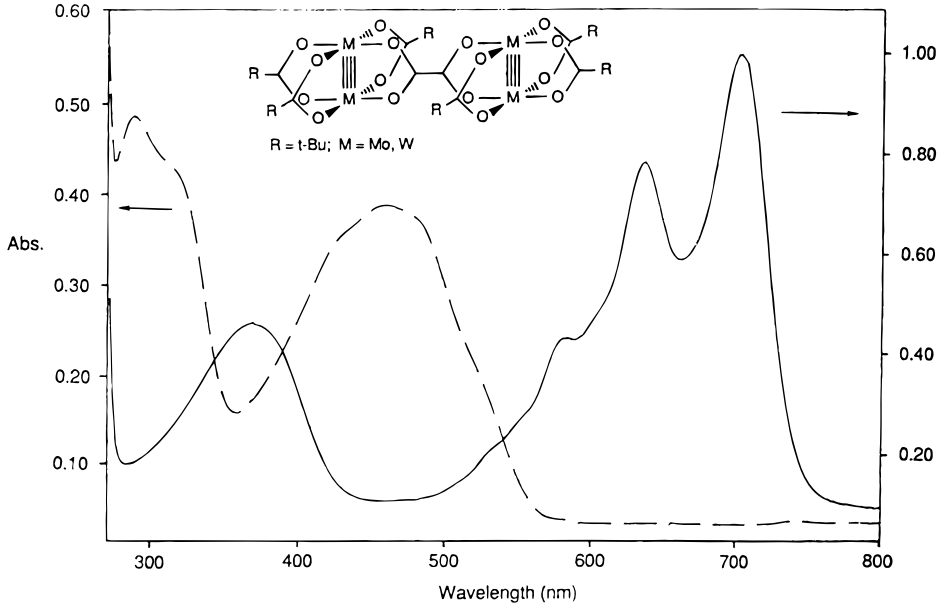


**FIGURE 3.** Electronic absorption spectra of $[M_2(O_2C^tBu)_3]_2(\mu$-oxalate) recorded in THF at room temperature.

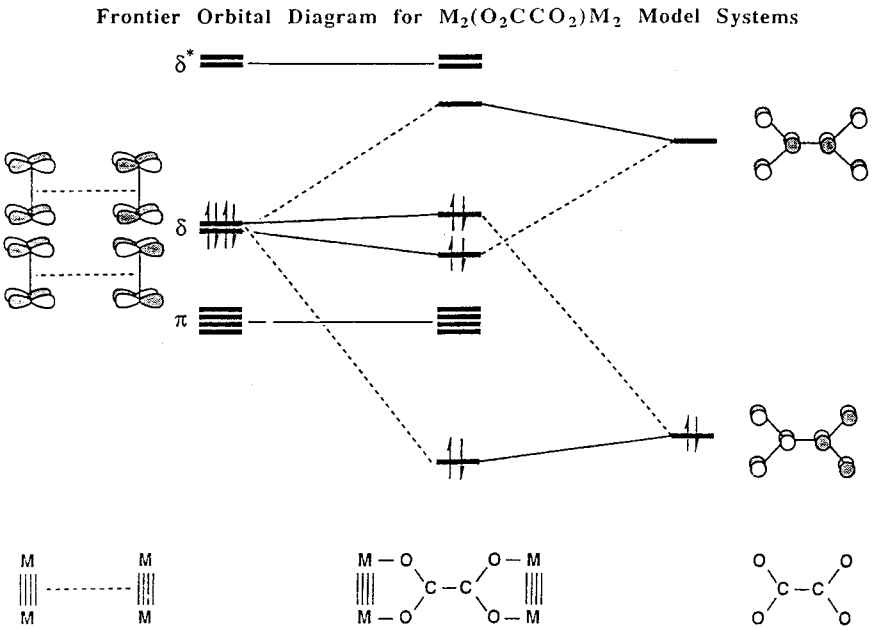


**FIGURE 4.** Qualitative MO diagram for oxalate-bridged $M_2$ quadruply bonded complexes showing the splitting of the two $\delta$ orbitals.

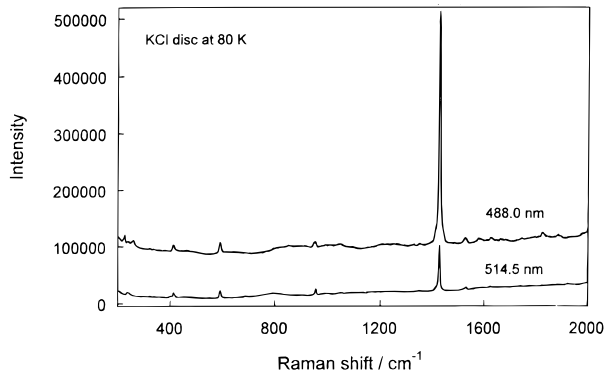


**FIGURE 5.** Raman spectrum of $[Mo_2(O_2C^tBu)_3]_2(\mu$-oxalate) ($Mo_4OXA$) recorded as a KCl disk at 80 K showing the resonance enhancement of the oxalate stretch at 1407 $cm^{-1}$ at 514.5 and 488.0 nm excitation. The corrected value of $\bar{\nu}$(Mo−Mo) is 397 $cm^{-1}$.

Support for this assignment comes from both computations and resonance Raman spectroscopy. The bonding in the linked dimers of "dimers" involves primarily the interactions of the two sets of $M_2$ $\delta$ orbitals and the filled $\pi$ and empty $\pi^*$ orbitals of the ligand bridge, as shown in Figure 4. The biggest difference between the $Mo_2$ and $W_2$ complexes arises from (i) the higher orbital energy of the $W_2$ $\delta$ orbitals and (ii) the stronger W−ligand bond. For this reason, the $W_2$ $\delta \rightarrow$ oxalate mixing is larger, and the $\delta \rightarrow$ oxalate $\pi^*$ transition is lower in energy.

The resonance Raman spectrum of $[Mo_2(O_2C^tBu)_3]_2(\mu$-oxalate) shows a strong resonance enhancement of $\nu(CO_2)$-(oxalate) at 1407 $cm^{-1}$ when the excitation is at 488 versus 514 nm[14] (see Figure 5). This is entirely consistent with the low-energy transition being a $M_2$ $\delta \rightarrow$ oxalate $\pi^*$ (MLCT) transition.

From the interaction diagram shown in Figure 4, one can easily extrapolate to the formation of a one-dimensional band structure. Because of $\delta$ and oxalate mixing, we obtain an oxalate $\pi^*$ conduction band and a filled-valence $\delta$ band. The optical band gap for the $W_2$−oxalate polymer is determined to be 1 eV,[12] and one can readily see the general implication that polymeric materials of types **A** and **B** will be semiconductors with tunable band gaps. Oxidation should yield one-dimensional conductors, and the attachment of a photoreceptor to the polymer backbone should yield one-dimensional photoconductive polymers.

**Electrochemical Studies.** Two limiting situations pertain to polymers of types **A** and **B** with respect to their redox properties. They may be either conductive or charge storage polymers. The electrochemical properties of the polymer may be investigated by cyclic voltammetry, and once again detailed studies of the linked dimers of "dimers" provide great insight.

Following the pioneering works of Taube, it is possible to define a conproportionation equilibrium constant, $K_c$, for the equilibrium shown in eq 4, based on the separation of the first and second oxidation potentials, which can be determined by cyclic voltammetry.[15]

$$[M_2\sim\sim\sim M_2] + [M_2\sim\sim\sim M_2]^{2+} \rightleftharpoons 2[M_2\sim\sim\sim M_2]^{+}, \quad K_c \quad (4)$$

$$\text{where} \qquad \ln K_c = \exp\left(\frac{\Delta E_{1/2}\,(\text{in mV})}{25.69}\right)$$

If there is no communication between the two $M_2$ centers, then a mixed-valence species, $[M_2^{+}\sim\sim\sim M_2^{0}]$, results, and excluding solvent and simple electrostatic effects, $K_c = 4.0$. On the other hand, if there is complete delocalization between the $M_2$ centers, as represented by $[M_2^{0.5+}\sim\sim\sim M_2^{0.5+}]$, then $K_c$ is very large, $\geq 10^6$. These two limiting situations of valence-trapped and fully delocalized are described as Class I and Class III, respectively, in the Robin and Day description of mixed-valence compounds.[16] The intermediate situation, in which there is electronic coupling but not full delocalization, is Class II, where typically $100 < K_c < 10^5$.

**Table 1. Summary of $K_c$ Values Determined by Cyclic Voltammetry for $[(^tBuCO_2)_3M_2(bridge)M_2(O_2C^tBu)_3]^+$ and Related $[(NH_3)_5M-bridge-M(NH_3)_5]^{5+}$ Complexes and the Classification According to the Robin and Day Scheme**

| compound[a] | $K_c$ | class |
|---|---|---|
| $Mo_2$ OXA $Mo_2$ | $5.4 \times 10^4$ | II |
| $W_2$ OXA $W_2$ | $1.3 \times 10^{12}$ | III |
| $Mo_2$ PFT $Mo_2$ | 36 | I |
| $W_2$ PFT $W_2$ | $6.6 \times 10^4$ | II |
| $Mo_2$ DAND $Mo_2$ | 62 | I |
| $W_2$ DAND $W_2$ | 290 | II |
| $W_2$ AND $W_2$ | 430 | II |
| $Mo_2$ DON $Mo_2$ | $2.0 \times 10^6$ | II or III |
| Ru pz Ru[b] | $3.9 \times 10^6$ | II or III |
| Os pz Os[b] | $7.0 \times 10^{12}$ | III |
| Ru 4,4′-bpy Ru[b] | 20 | I |
| Os 4,4′-bpy Os[b] | 600 | II |

[a] OXA = oxalate; PFT = perfluoroterephthalate; DAND = 9,10-dihydro-1,8-anthracenyldicarboxylate; AND = 1,8-anthracenyldicarboxylate; DON = 2,7-dioxynaphthyridine; pz = pyrazine; 4,4′-bpy = 4,4′-bipyridine. [b] Data taken from ref 15b.

The oxalate-bridged $[W_2]_2$ pivalate complex reveals two single-electron oxidation waves separated by ca. 0.8 V, indicating a very strong electronic communication, $K_c \approx 10^{12}$. Also, the first oxidation is fully reversible and occurs at a potential 0.5 V lower than that of $W_2(O_2C^tBu)_4$.[12] This is clearly in full agreement with the MO interaction diagram in Figure 4, which shows that the oxalate bridge raises the energy of one of the $\delta$ orbitals by a filled−filled interaction. The mixing of $M_2$ $\delta$ and oxalate orbitals is notably weaker for molybdenum, and the separation of the first and second oxidation potentials is less, leading to $K_c \approx 10^5$.[12]

A summary of $K_c$ values for certain bridged dimers of "dimers" is given in Table 1, where a comparison is also made with the related Taube $[(NH_3)_5M(bridge)-M(NH_3)_5]^{4+/5+/6+}$ systems (M = Ru, Os). Two important similarities are seen. (1) The electronic coupling is greater for the third row transition elements M = Os and W than for their second row analogues. This is understandable in terms of the orbital energies of the Os/Ru $t_{2g}$ and $W_2$/$Mo_2$ $\delta$ orbitals, which leads to better M $d_\pi$−ligand $\pi^*$ orbital interactions for the third row transition elements. (2) With increasing distance between the interacting metal centers, the electronic communication falls off. Compare the data for pyrazine with those for 4,4′-bipyridine and the data for oxalate with those for perfluoroterephthalate, for example.

There is, however, one other important point to note from the data presented in Table 1. Even though the $M_2$- - -$M_2$ separation in parallel linked dimers of "dimers" is ca. 3.0 Å (as determined by crystallography and shown in Figure 2), the value of $K_c$, the measure of the electronic coupling, is dependent on the extent of the $M_2$ $\delta \rightarrow$ bridge $\pi^*$ interaction. So, for 2,7-dioxynaphthyridine there is strong coupling, but for 1,8-anthracenedicarboxylate bridges the coupling is only weak. Even though parallel-linked polymers may give the appearance of being ideally set up to form a molecular wire, the electronic communication still occurs via the ligand bridge. The net conclusion to be made from the above is that electronic communication is favored by maximizing $M_2$ $\delta \rightarrow$ bridge $\pi^*$ interactions and the shorter $M_2-M_2$ distances. It is, therefore, of note that the dioxypyridazine ligand-bridged complex shown in **F** below yields the highest value of $K_c$ and the strongest electronic coupling.[17]

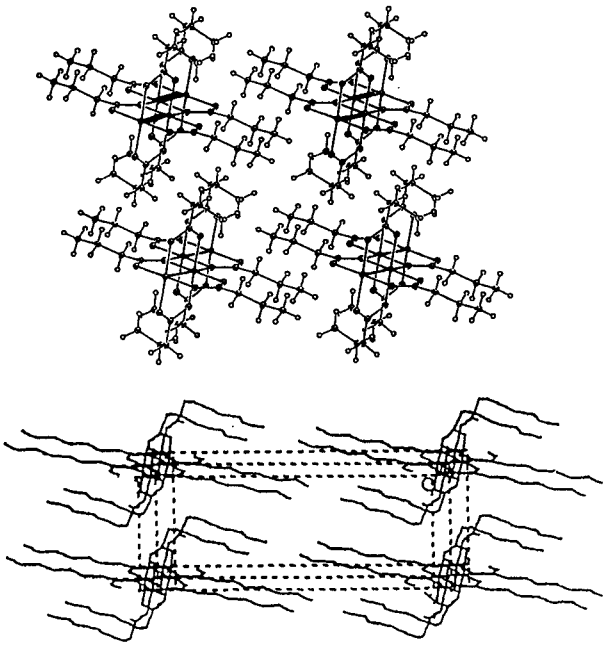

**FIGURE 6.** Packing diagrams of two unit cells of $W_2(O_2C(CH_2)_2CH_3)_4$ (top) and $Cu_2(oct)_4$ (bottom).

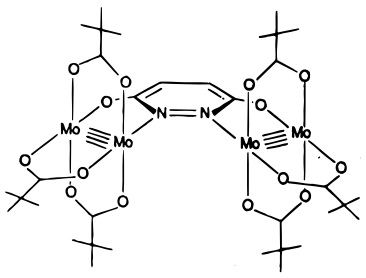

**F**

**Columnar Mesophases.** The alignment of M−M axes in the solid state can be achieved either through the weak packing forces of the ligands or by intermolecular metal−ligand atom interactions. An example of the former is seen in the structure of $W_2(OCy)_6$, where Cy = cyclohexyl. Here, the cyclohexyl ligands form a packing motif which leads to the alignment of the M−M axes but with no short intermolecular $M_2$- - -$M_2$ distances.[18] As examples of the second type of alignment, one can inspect the structures of $W_2(O_2C_2Me_4)_3$[18] and $M_2(O_2CR)_4$ compounds.[4] Here, weak intermolecular (- -$Mo_2$- - -O- - -$Mo_2$- -)$_\infty$ bonds cause laddered structures where infinite chains run parallel to one another. Drawings depicting two unit cells of the $W_2(O_2C(CH_2)_2CH_3)_4$ and $Cu_2(O_2C(CH_2)_6CH_3)_4$ structures are shown in Figure 6. The *n*-alkanoates, $M_2(O_2CR)_4$, where M = Cr, Mo, W, Ru, Rh, and Cu, adopt a common structure in the solid state involving a triclinic unit cell, where *c*, the short axis of chain propagation, is ca. 5.6 Å, $b$ = 8.5 Å, and $a$ is a distance dependent on the number

**Table 2. Unit Cell Lattice Constant Distances for $Mo_2(O_2C(CH_2)_nCH_3)_4$ Calculated from X-ray Powder Diffraction Patterns and Intercolumnar Distances in the Mesophase *d* (Å)**

| | | lattice constants (*d*, Å) | | | |
|---|---|---|---|---|---|
| compound | cell type | *a* | *b* | *c* | *d* |
| $Mo_2(O_2C(CH_2)_2CH_3)_4$ | tricl | 11.14 ± 0.04 | 8.856 ± 0.03 | 5.593 ± 0.017 | – |
| $Mo_2(O_2C(CH_2)_3CH_3)_4$ | tricl | 13.59 ± 0.06 | 8.46 ± 0.03 | 5.604 ± 0.01 | 13.3 |
| $Mo_2(O_2C(CH_2)_4CH_3)_4$ | tricl | 16.61 ± 0.03 | 8.642 ± 0.01 | 5.592 ± 0.007 | 14.2 |
| $Mo_2(O_2C(CH_2)_6CH_3)_4$ | tricl | 21.31 ± 0.03 | 8.593 ± 0.01 | 5.551 ± 0.006 | 16.3 |
| $Mo_2(O_2C(CH_2)_7CH_3)_4$ | tricl | 24.67 ± 0.02 | 7.788 ± 0.01 | 5.558 ± 0.005 | 17.x |

**Table 3. Thermotropic Properties of a Series of Dimetal Tetraoctanoates**

| M | n | Phase Profile [T°C (ΔH, kcal/mol)][a] |
|---|---|---|
| Cr | 6 | K ⟷ 99° (10.1) ⟷ LC ⟶ >300° ⟶ Dec |
| Mo | 6 | K ⟷ 100° (13.6) ⟷ LC ⟷ 147° (0.6) ⟷ IL |
| W | 6 | K ⟷ 90° (13.7) ⟷ IL |
| Ru | 6 | K ⟷ 107° (12.0) ⟷ LC ⟶ >290° ⟶ Dec |
| Rh[b] | 6 | K ⟷ 95° (6.6) ⟷ LC ⟶ >220° ⟶ Dec |

[a] Marchon and co-workers. *J. Phys. Chem.* **1986**, *90*, 5502. [b] K = crystal; LC = mesophase; IL = isotropic liquid; Dec = decompose

of methylene units, *n*, for R = $(CH_2)_nCH_3$.[19] A representative listing of cell parameters is given in Table 2. The thermotropic behavior of this class of compounds, having the molecular paddle-wheel motif shown in **A**, depends on the nature of *n* and M. The thermotropic properties of a series of octanoates are given in Table 3, and the data reveal the important role of M. The existence of the mesophase and its temperature range correlates with the relative strength of the intermolecular $M_2$- - -O interactions. These are inversely proportional to the trans influence (and bond strength) of the $M^{n}M$ bond. In the case of $Cu_2^{4+}$, there is no formal Cu-to-Cu bond, and the long axial Cu−O bonds may merely be thought of as arising from a Jahn−Teller distortion. The remarkable difference in the thermotropic behavior of the group 6 metal tetraoctanoates reflects the relative strength of the M−M quadruple bonds: W > Mo ≫ Cr.

The thermotropic behavior can be monitored by differential scanning calorimetry, which reveals that these compounds exhibit reversible phase changes. For molybdenum, the temperature range of the mesophase can be dramatically altered by alkyl chain side-branching and by the use of perfluoroalkyl carboxylates.[19]

By optical microscopy, the mesophases show fan-shaped or conical textures typical of discotic or columnar mesophases, and low-angle X-ray diffraction studies support the assignment of the mesophase as hexagonal columnar with an intercolumnar separation that increases with increasing *n* for R = $(CH_2)_nCH_3$. The coherence length within a column can be estimated to be ca. 35 Å and the plane-to-plane separation ca. 4.7 Å.[19]

From the photomicrographs and the low-angle X-ray data, it is possible to formulate a molecular model for the mesophase as shown in Figure 7. The crystal to mesophase transition involves a loss of order of the packing of the *n*-alkyl groups accompanied by rapid and reversible dissociation of the weak intermolecular $Mo_2$- - -O bonds. Thus, rapid and reversible $C_4$ and $C_2$ (glide) motions generate a hexagonal columnar (rather than a tetragonal columnar) packing of columns in the mesophase. Above the clearing temperature, the ordering arising from the weak intermolecular $M_2$- - -O interactions is lost. Since $M_2$- - -O interactions are stronger for M = Cr than Mo, the clearing temperature is higher for M = Cr as, indeed, it is for M = Ru, Rh, and Cu, which also have shorter and stronger $M_2$- - -O interactions. There are important physical characteristics of these mesophases that are directly explained by this dynamic molecular model (Figure 7).

**Alignment of the Mesophase in a Magnetic Field.** The free energy, *G*, of alignment of a molecule in a magnetic field is given by eq 5, where α is the angle between the director and the applied magnetic field and $\Delta\chi = \chi_{II} - \chi_{\perp}$, the anisotropy of the susceptibility.[20]

$$G = -\Delta\chi H^2 (3\cos^2\alpha - 1)/6 \qquad (5)$$

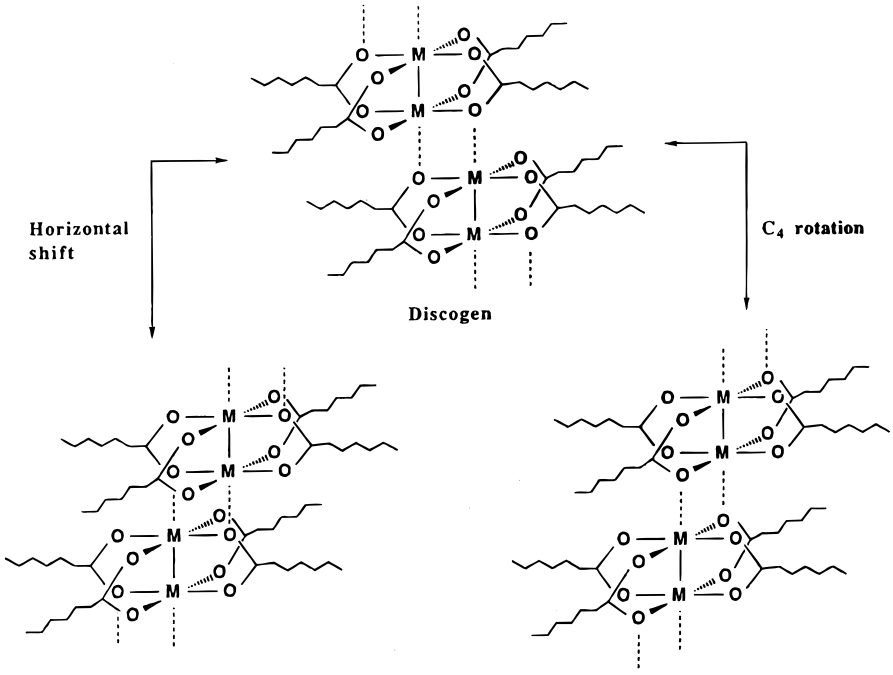


**FIGURE 7.** Model of the motions of the $Mo_2(O_2C)_4$ core in the mesophase of $Mo_2(O_2CR)_4$ compounds.

When $\Delta\chi$ is positive, $G$ is minimized for $\alpha = 0$ with the director parallel to the applied magnetic field $H$. When $\Delta\chi$ is negative, $G$ is minimized for $\alpha = 180°$ with the director perpendicular to $H$. Given that the magnetic anisotropy of a M−M quadruple bond is large and negative,[10] we would expect that $M_2(O_2CR)_4$ compounds (M = Mo and W) would align themselves perpendicular to an applied magnetic field. This has been confirmed by examining the $^{13}C$ NMR spectra of the isotopically labeled $Mo_2(O_2{}^{13}C(CH_2)_6CH_3)_4$ compound.[19]

The broad-line solid-state $^{13}C$ spectrum of the carboxylate 13-carbon leads to the values $\sigma_{xx} = 220$ ppm, $\sigma_{yy} = 209$ ppm, and $\sigma_{zz} = 124$ ppm for the three chemical shift tensors as shown in **G**. These values are shifted somewhat

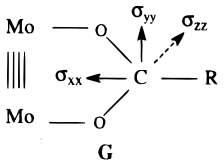


**G**

from typical carboxylate values (e.g.,[21] $\sigma_{xx} = 245$, $\sigma_{yy} = 177$, and $\sigma_{zz} = 105$ ppm) because of the magnetic influence (anisotropy) of the Mo−Mo quadruple bond.[10]

In the isotropic liquid phase, a single resonance is observed at $\delta$ 183, which compares well with that expected from the average: $(\sigma_{xx} + \sigma_{yy} + \sigma_{zz})/3 = 184$ ppm. Upon cooling of the mesophase to 125 °C, a single, slightly broadened resonance is observed at $\delta$ 169. This chemical shift does not correspond to $\sigma_{yy}$, thereby indicating that the M−M axes within the columns are not aligned parallel to the magnetic field. The value of $\delta$ 169 corresponds closely to $(\sigma_{xx} + \sigma_{zz})/2 = 172$ ppm based on the solid-state spectrum. This is, therefore, consistent with the columnar axis being aligned perpendicular to the applied magnetic field and a rapid and reversible breaking of the $Mo_2$- - -O bonds. This has the effect, by $C_4$ and $C_2$ rotations, of allowing the $M_2$ units to align within the parallel columns that stack in a hexagonal manner.

**Viscoelastic Properties.** The complex viscosity, $\eta^*$, can be related to the oscillatory storage modulus $G'$, the loss modulus $G''$, and the angular frequency of oscillation $\omega$, according to eq 6.[22]

$$\eta^* = \frac{\sqrt{(G')^2 + (G'')^2}}{\omega} \tag{6}$$

A comparison of the rheological properties of the $M_2(O_2C(CH_2)_6CH_3)_4$ complexes, where M = Mo and Cu, is most instructive, for it reveals two important features of this class of mesogens.[23] **(**1) At constant $\omega$, the complex viscosity $\eta^*$ decreases slightly with increasing temperature. However, for M = Mo there is a precipitous drop in viscosity at the clearing temperature. Also, within the liquid crystal phase, the $Cu_2$ octanoate is an order of magnitude more viscous than the $Mo_2$ analogue. This can be related to the stronger (and shorter) axial $M_2$- - -O interactions within the columns that are present for M = Cu relative to M = Mo. As noted before, these $M_2$- - -O interactions are inversely proportional to the trans influence and trans effect exerted by the M−M interaction. For M = Cu there is no M−M bond; the metal atoms are merely antiferromagnetically coupled.[24] (2) While the viscosity of these dimetal octanoates is typical of a molten polymer such as polypropylene with a $M_w$ of ca. $10^6$ Da, the viscoelastic response of such compounds as a function of $\omega$ (radians per second) is distinctly nonlinear, yet reversible. With increasing $\omega$, the values of $\eta^*$ drop off for both M = Mo and Cu in a closely related manner at $T =$ 125 °C. This phenomenon is completely reversible and is not characteristic of a hydrocarbon polymer or an oil that would be used as a lubricant in a motor engine. However,

this nonlinear viscosity as a function of $\omega$ can be related to the molecular behavior within the mesophase. As noted before, there is evidence that the $M_2$- - -O bonds are being broken and re-formed rapidly within the mesophase. Thus, with increasing $\omega$, the columns are mechanically "chopped up", resulting in a drop in viscosity, but as $\omega$ decreases the $M_2$- - -O bonds re-form, the columnar phase regains its order, and the viscosity increases.

**Mixtures.** The mixtures of octanoates, nonanoates, and dodecanoates follow behavior that can be anticipated by the Schroder van Lauer equation;[25] i.e., they behave approximately as expected for ideal mixtures.[26] In contrast, the thermotropic behavior of mixtures of $Mo_2(O_2C(CH_2)_6CH_3)_4$ and $Mo_2(O_2C(CF_2)_6CF_3)_4$ is far from ideal. This is not surprising because hydrocarbon and fluorous phases are normally immiscible.[27] What is surprising is that a 1:1 mixture of $Mo_2(O_2C(CH_2)_6CH_3)_4$ and $Mo_2(O_2C(CF_2)_6CF_3)_4$ forms a homogeneous co-mesophase.[26] Photomicrographs reveal the fan-shaped textures associated with the columnar mesophases of the homoleptic $M_2$ carboxylates. Seemingly, the only reasonable explanation for this unusual mixing of a fluorous phase and a hydrocarbon phase is that ligand scrambling occurs (eq **7)**, and this allows for complete miscibility of the species present in the mesophase formed upon cooling from the isotropic liquid phase.

$$Mo_2(O_2CR)_4 + Mo_2(O_2CR_f)_4 \rightleftharpoons Mo_2(O_2CR_f)_{4-n}(O_2CR)_n \quad (n = 0-4) \quad (7)$$

Reaction 7 has been noted in solution for these systems and has been shown to arise from catalysis due to the presence of trace quantities of $H^+$ and $O_2CR^-$.[28]

We have also studied mixtures of $Mo_2(O_2{}^{13}C(CH_2)_6CH_3)_4$ and $Ru_2(O_2{}^{13}C(CH_2)_6CH_3)_4$ by $^{13}C$ NMR spectroscopy.[29] The $Ru_2^{4+}$ center is paramagnetic with a triplet ground state: M−M configuration $\sigma^2\pi^4\delta^2\delta^{*2}\pi^{*2}$.[4] We have examined the solution behavior of $Ru_2$(octanoates)$_4$ by $^1H$ and $^{13}C\{^1H\}$ NMR spectroscopy, which is informative with regard to $Ru_2$- - -O interactions and the formation of $[Ru_2]_n$ oligomers in solution.[30] It is therefore of particular interest to note that, while $Mo_2^{4+}$ and $Ru_2^{4+}$ octanoates, separately and together, form a mesophase in the temperature range 100−145 °C, the $^{13}C$ NMR spectrum of the $Mo_2(O_2{}^{13}C(CH_2)_6CH_3)_4$ carboxylate carbon indicates that the columns involve exclusively $[Mo_2]_n$ units.[29] Conversely, the $[Ru_2^{4+}]_n$ units associate.[29] This can be understood in terms of the strength of the $[Ru_2^{4+}]$- - -O interactions being considerably greater than that of the $[Mo_2^{4+}]$- - -O interactions, such that the formation of the columnar phase may be viewed akin to the formation of a polymer where Markovian statistics apply.[31]

**Concluding Remarks.** Cotton and co-workers[4] have shown that multiple bonds between metal atoms are accessible for the vast majority of transition metal elements when bridging ligands are employed of the type schematically represented by **H**, when X, Y, and Z are combinations of C, N, and O. The use of such ligands is testimony to the great possibilities that exist for making extended chains of $M_2$ units bridged by ligands such as

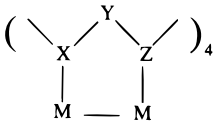


**H**

oxalate, perfluoroterephthalate, etc. Recently, Cotton and Murillo have prepared and structurally characterized linked dimers, trimers, and tetramers employing formamidinato-supported $M_2^{4+}$ centers, where M = Mo and Rh.[32] The opportunities for incorporating $M_2$ units into extended chains seem limited only by one's imagination.

In the area of incorporating M−M multiple bonds into mesogens, much still remains to be done. It will be interesting to see whether charged species $Mo_2(O_2CR)_4{}^+X^-$ can be incorporated into the columns. Such species could yield a one-dimensional metallic columnar mesophase. Also, of particular interest are the nonlinear optical responses of these phases.[11] From our present work, we know that they are uniaxially positive materials[26]—light travels faster down the M−M columnar axis than it does perpendicular to the columns. The study of the optical properties of the aligned mesophases thus presents a challenge for future investigations.

It is, however, wise, when contemplating potential applications of metalloorganic polymers and metallomesogens, to recall the following words: "oft expectation fails, and most oft there where most it promises...".[33]

*I thank the National Science Foundation for support of this work and many talented co-workers and collaborators cited in the references. This Account is based in part upon the 12th Annual Geoffrey Coates Lecture, University of Wyoming, March 1999.*

## References

(1) *Metallomesogens: Synthesis, Properties and Applications*; Serrano, J. L., Ed.; VCH Weinheim: New York, Basel, Cambridge, Tokyo, 1996.

(2) (a) Cayton, R. H.; Chisholm, M. H. Electronic Coupling Between Covalently Linked Metal−Metal Quadruple Bonds of Molybdenum and Tungsten. *J. Am. Chem. Soc.* **1989**, *111*, 8921−8923. (b) Cayton, R. H.; Chisholm, M. H.; Huffman, J. C.; Lobkovsky, E. B. Mo−Mo Quadruple Bonds Bridged by 1,8-Naphthyridinyl-2,7-Dioxides. An Insight into the Nature of a Parallel-Linked Stiff-Chain Polymer: $[\sim\sim\sim(M\text{-}4\text{-}M)\sim\sim\sim(M\text{-}4\text{-}M)\sim\sim\sim]_x$. *Angew. Chem., Int. Ed. Engl.* **1991**, *30*, 862−864.

(3) Cayton, R. H.; Chisholm, M. H.; Darrington, F. D. Multiple Bonds Between Metal Atoms in Ordered Assemblies: Liquid Crystals Containing Quadruple Bonds Between Molybdenum Atoms. *Angew. Chem., Int. Ed. Engl.* **1990**, *29*, 1481−1483.

(4) Cotton, F. A.; Walton, R. A. *Multiple Bonds Between Metal Atoms*, 2nd ed.; Oxford University Press: Oxford, UK, 1993.

(5) (a) Xie, Y.; Grev, R. S.; Gu, J.; Schaeffer, H. F., III; Schleyer, P. v. R.; Su, J.; Li, X.-W.; Robinson, G. H. The Nature of the Gallium−Gallium Triple Bond. *J. Am. Chem. Soc.* **1998**, *120*, 3773−3780. (b) Cotton, F. A.; Cowley, A. H.; Feng, X. The Use of Density Functional Theory to Understand and Predict Structures and Bonding in Main Group Compounds with Multiple Bonds. *J. Am. Chem. Soc.* **1998**, *120*, 1795−1799.

(6) Lichtenberger, D. L. Experimental Measures of Metal−Metal Sigma, Pi and Delta Bonding from Photoelectron Spectroscopy. In *Metal−Metal Bonds and Clusters in Chemistry and Catalysis*; Fackler, J. P., Ed.; Plenum Press: 1990; pp 275−298.

(7) (a) Martin, D. S.; Newman, R. A.; Fanwick, P. E. Polarized Electronic Absorption Spectra of Dimolybdenum (II) Tetraacetate. *Inorg. Chem.* **1979**, *18*, 2511−2520. (b) Cotton, F. A.; Zhong, B. The Polarized Single-Crystal Visible Spectrum of $Mo_2(O_2CPh)_4$. *J. Am. Chem. Soc.* **1990**, *112*, 2256−2260.

(8) Chisholm, M. H.; Huffman, J. C.; Iyer, S. S.; Lynn, M. A. Nitro-Substituted Benzoates of Dimolybdenum: The $Mo_2^{4+}$ $\delta$ to Ligand Charge-Transfer Band. *Inorg. Chim. Acta* **1996**, *243*, 283−293.

(9) Chisholm, M. H.; Clark, D. L.; Huffman, J. C.; Van Der Sluys, W. G.; Kober, E. M.; Lichtenberger, D. L.; Bursten, B. E. The Tungsten−Tungsten Triple Bond. XIII. Bisalkyltetra-carboxylates of Dimolybdenum and Ditungsten. Triple Bonds Between Metal Atoms with the Valence M.O. Description $\pi^4\delta^2$. *J. Am. Chem. Soc.* **1987**, *109*, 6796−6816.

(10) (a) Reference 4; Section 10.1.7 and references therein. (b) Cotton, F. A.; Kitagawa, S. Diamagnetic Anisotropy of Quadruple Mo−Mo Bonds: α-$Mo_2Cl_4$(diphosphine)$_2$ Complexes. *Polyhedron* **1989**, *7*, 1673−1676.

(11) Mashima, K.; Tanaka, M.; Kaneda, Y.; Fukumoto, A.; Mizomoto, H.; Tani, K.; Nakono, H.; Nakamura, A.; Sakaguchi, T.; Kamada, K.; Ohta, K. Large Third-Order Nonlinear Optical Susceptibilities of Multiply Bonded $M_2$(pyphos)$_4$ and $M_2Pd_2Cl_2$(pyphos)$_4$ (M = Cr, Mo; Pyphos = 6-phenylphosphino-2-pyridonate) By Picosecond Degenerate Four-Wave Mixing Method. *Chem. Lett.* **1997**, 411−412.

(12) (a) Cayton, R. H.; Chisholm, M. H.; Huffman, J. C.; Lobkovsky, E. B. Metal−Metal Multiple Bonds in Ordered Assemblies. 1. Tetranuclear Molybdenum and Tungsten Carboxylates Involving Covalently Linked M−M Quadruple Bonds. Molecular Models for Subunits of One-Dimensional Stiff-Chain Polymers. *J. Am. Chem. Soc.* **1991**, *113*, 8709−8724. (b) Cayton, R. H.; Chisholm, M. H., results to be published.

(13) Cotton, F. A.; Lin, C.; Murillo, C. A. Coupling $Mo_2^{n+}$ Units via Dicarboxylate Bridges. *J. Chem. Soc., Dalton Trans.* **1998**, 3151−3153.

(14) Chisholm, M. H.; Macintosh, A. M.; Clark, R. J. L.; Firth, S., results to be published.

(15) (a) Creutz, C.; Taube, H. Binuclear Complexes of Ruthenium Amines. *J. Am. Chem. Soc.* **1973**, *95*, 1086−1094. (b) Creutz, C. Mixed Valence Complexes of $d^5$-$d^6$ Metal Centers. *Prog. Inorg. Chem.* **1983**, *30*, 1−73. (c) Ward, M. Metal−Metal Interactions in Binuclear Wires and Switches. *Chem. Soc. Rev.* **1995**, 121−134.

(16) Robin, M. B.; Day, P. Mixed Valence Chemistry—A Survey and Classification. *Adv. Inorg. Radiochem.* **1967**, *10*, 247−422.

(17) Cayton, R. H.; Chisholm, M. H.; Putilina, E. F.; Folting, K. Covalently Linked Molybdenum−Molybdenum Quadruple Bonds. Dioxypyridizine Dianion and 2-Imidazolinethionate as Bridges Between Molybdenum Fragments. *Polyhedron* **1993**, *12*, 2627−2633.

(18) Chisholm, M. H.; Folting, K.; Hampden-Smith, M. J.; Smith, C. A. Preparation and Characterization of Hexacyclohexoxides and Trispinacolato-ditungsten (M≡M). A Comparison of Staggered and Ethane-like $O_3W{\equiv}WO_3$ Units. *Polyhedron* **1987**, *6*, 1747−1755.

(19) Baxter, D. V.; Cayton, R. H.; Chisholm, M. H.; Huffman, J C.; Putilina, E. F.; Tagg, S. L.; Wesemann, J. L.; Zwanziger, J. W. Multiple Bonds in Ordered Assemblies. 2. Quadruple Bonds in the Mesomorphic State. *J. Am. Chem. Soc.* **1994**, *116*, 4551−4566.

(20) Emsley, J. W.; Lindon, J. C. *NMR Spectroscopy Using Liquid Crystalline Solvents*; Pergamon Press: New York, 1975.

(21) (a) Veeman, W. S. *Prog. NMR Spectrosc.* **1984**, *16*, 193. (b) Duncan, T. M. *J. Phys. Chem. Ref. Data* **1987**, *16*, 125.

(22) Ferry, J. D. *Viscoelastic Properties of Polymers*; J. Wiley Publishers: New York, 1980.

(23) Mackley, M. R.; Marshall, R. J. J.; Chisholm, M. H.; Putilina, E. F. A Rheological Study of the Mesomorphic State of Dimolybdenum and Dicopper Octanoates. *Chem. Mater.* **1995**, *7*, 1938−1941.

(24) (a) Bleaney, B.; Bowers, K. D. Anomalous Paramagnetism of Copper Acetate. *Proc. R. Soc. (London) A* **1952**, *214*, 451−465. (b) Bleaney, B.; Bowers, K. D. Anomalous Paramagnetism and Exchange Interaction in Copper Acetate. *Philos. Mag.* **1952**, *43*, 372−374.

(25) Schroder, I. Ügber die Abhängigkeit der Löslichkeit eines festen korpers von seiner Schmelztemperatur. *Phys. Chem.* **1893**, *11*, 449−465.

(26) Baxter, D. F.; Chisholm, M. H.; Lynn, M. A.; Putilina, E. F.; Trzaska, S. T.; Swager, T. Studies of Thermotropic Properties and the Mesophase of Mixtures of n-Alkanoates and Perfluoro-n-alkanoates of Dimolybdenum. *Chem. Mater.* **1998**, *10*, 1758−1763.

(27) This forms the theme of a current area of catalysis involving biphasic media. See: Guillevic, M.-A.; Arif, A. M.; Horváth, I. T.; Gladycz, J. A. Synthesis, Structure and Oxidative Additions of a Fluorous Analogue of Vaska's Compound—Altered Reactivity in Fluorocarbons and Implications for Catalysis. *Angew. Chem., Int. Ed. Engl.* **1997**, *36*, 1612−1614.

(28) Chisholm, M. H.; Macintosh, A. M. On the Mechanism of Carboxylate Scrambling at $Mo_2^{4+}$ Centers: Evidence for a Catalyzed Mechanism. *J. Chem. Soc., Dalton Trans.* **1999**, 1205−1207.

(29) Chisholm, M. H.; Wesemann, J. L.; Zwanziger, J. W., results to be published.

(30) (a) Chisholm, M. H.; Christou, G.; Folting, K.; Huffman, J. C.; James, C. A.; Samuels, J. A.; Wesemann, J. L.; Woodruff, W. H. Solution Studies of $Ru_2(O_2CR)_4^{n+}$ Complexes, where n = 0 and 1 and $O_2CR$ = Octanoate, Crotonoate, Dimethylacrylate, Benzoate and p-Tolunate) and Solid-State Structure of $Ru_2(O_2C$-p-tolyl$)_4$-$(THF)_2$, $Ru_2(O_2C$-p-tolyl$)_4(THF)_2^+BF_4^-$, and $Ru_2(O_2C$-p-tolyl$)_4(CH_3$-$CN)_2$: Investigation of the Axial Ligation on the $Ru_2$ Core. *Inorg. Chem.* **1996**, *35*, 3643−3658. (b) Wesemann, J. L.; Chisholm, M. H. Incorporation of $Ru_2(O_2C(CH_2)_6CH_3)_4$ into Extended Chains: Interaction of $Ru_2(O_2C(CH_2)_6CH_2)_4$ with Pyrazine, 4-Cyanopyridine, TCNE and Benzoquinone. *Inorg. Chem.* **1997**, *36*, 6, 3258−3267. (c) Chisholm, M. H.; Folting, K.; Moodley, K. G.; Wesemann, J. L. Further Comments on the Lability of $M_2(O_2CR)_4$ Complexes and the Structural Characterization of $[Bu_4nN^+]_2[Rh_8(O_2C^tBu)_{16}(O_2CMe)_2$-$(toluene)_2]^{2-}$. *Polyhedron* **1996**, *15*, 1903−1905.

(31) Bovey, F. A. *Chain Structure and Conformation of Macromolecules*; Academic Press: New York, 1982.

(32) (a) Cotton, F. A.; Daniels, L. M.; Lin, C.; Murillo, C. A. The Designed "Self-Assembly" of a Three-Dimensional Molecule Containing Six Quadruply-Bonded $Mo_2^{4+}$ Units. *Chem. Commun.* **1999**, 841−842. (b) Cotton, F. A.; Daniels, L. M.; Lin, C.; Murillo, C. A. Square and Triangular Arrays Based on $Mo_2^{4+}$ and $Rh_2^{4+}$ Units. *J. Am. Chem. Soc.* **1999**, *121*, 4538−4539.

(33) Shakespeare, W. *All's Well That Ends Well*; II, i, 145−6.

AR9800901